The structure of the stoichiometric and reduced SnO₂(110) surface

I. Manassidis, J. Goniakowski, L.N. Kantorovich, M.J. Gillan *

Physics Department, Keele University, Keele, Staffordshire ST5 5BG, UK

Received 14 April 1995; accepted for publication 24 May 1995

Abstract

First-principles calculations based on density functional theory (DFT) and the pseudopotential method have been used to study the stoichiometric and reduced SnO₂(110) surface. The ionic relaxations are found to be moderate for both the stoichiometric and reduced surfaces, and are very similar to those found in recent DFT-pseudopotential work on TiO₂. Removal of neutral oxygen leaves two electrons per oxygen on the surface, which are distributed in channels passing through bridging oxygen sites. The associated electron density can be attributed to reduction of tin from Sn^{4+} to Sn^{2+}, but only if the charge distribution on Sn^{2+} is recognized to be highly asymmetric. Reduction of the surface gives rise to a broad distribution of gap states, in qualitative agreement with spectroscopic measurements.

Keywords: Ab initio quantum chemical methods and calculations; Density functional calculations; Low index single crystal surfaces; Tin oxides

1. Introduction

Stannic oxide (SnO_2) is a wide-gap semiconductor ($E_g = 3.6$ eV [1]) which is used in gas-sensing devices [2], and is also of interest as an oxidation catalyst [3]. These applications have stimulated intensive study of its surface properties [4–17], concentrating mainly on the (110) surface (see Fig. 1), which is the most stable. Because of the variable valence of Sn, the material readily loses surface oxygen, and there have been a number of studies of the atomic structure, electronic structure and electrical properties of the (110) surface as a function of temperature and oxygen partial pressure. The existence of a rather complicated series of surface reconstructions [4,10,13], marked changes of electronic structure in the band gap [5,9,12], and strong variation of the surface electrical conductivity with deviation from stoichiometry [9,13] are all well documented. In spite of this work, many questions remain unresolved. For example, there is no experimental information about the energetics of the surface, or about the nature of surface relaxations. Nor is there a clear picture at present of the electronic charge density at the surface, and the way this is modified by removal of oxygen. The detailed interpretation of the observed gap states also remains controversial.

The aim of the present work is to use first-principles calculations to build up a detailed picture of the energetics, atomic structure and electronic structure of both the stoichiometric and the reduced SnO₂(110) surface. We report calculated results for the energy
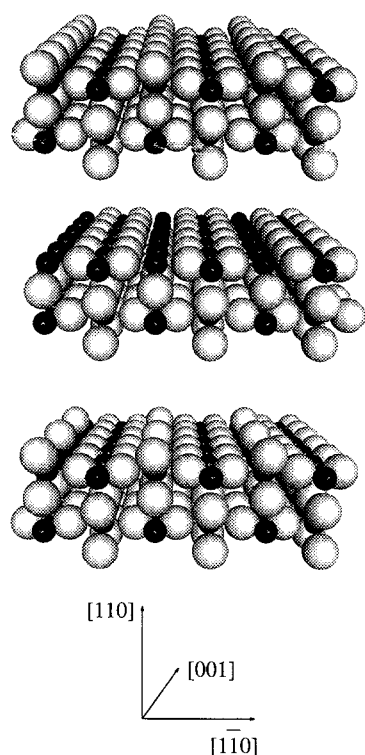
---

* Corresponding author. E-mail: pha71@keele.ac.uk.

Fig. 1. Perspective view of the stoichiometric (upper panel), fully reduced (middle) and half-reduced (lower) surfaces of SnO_2. Small dark spheres and large light spheres represent Sn and O respectively.

of the relaxed and unrelaxed surfaces, the relaxed atomic positions, the valence electron distribution and the surface electronic density of states. The calculations have been performed using density functional theory (DFT) and the pseudopotential technique [20,21,22]. These methods have a growing record of success in studying a wide range of oxides, including MgO [23,24], Li_2O [25], Al_2O_3 [26,27], SiO_2 [28] and TiO_2 [29,30], and have been used to investigate the structure and energetics of lattice defects and surfaces of oxide materials, and the process of molecular adsorption on their surfaces [31]. In a previous paper [32], we have reported a detailed investigation of the SnO_2 and SnO perfect crystals using the present methods. We showed there that the calculations account satisfactorily for the equilibrium crystal structure, phonon frequencies and electronic structure of the two materials, and those investigations form the basis for the present work.

When considering the structure of oxide surfaces, it is important to recall the very great differences that exist between different surfaces. At one extreme, there is the almost complete lack of relaxation effects revealed both by experiments [33–35] and by ab initio calculations [31,36] for the case of the MgO(001) surface; at the other, there are the very large atomic relaxations leading to a major reduction in surface energy found on the α-alumina basal-plane surface [26,27]. In this context, we shall see that $SnO_2(110)$ is an intermediate case, showing only moderate deviations from bulk termination. Even the gross disturbance associated with loss of surface oxygen will be shown to lead to only rather minor displacements.

A particularly important aspect of the present work concerns the spatial distribution of valence electrons at the surface. On a simple ionic picture, removal of neutral oxygen would lead to the reduction of tin from the Sn^{4+} to the Sn^{2+} state, and spectroscopic studies have given support to this [12]. Alternatively, we might regard the removal of neutral oxygen as creating surface F-centres. On the first view, we would expect the electrons left on the surface to be concentrated on surface Sn ions. The second view might lead us to expect electrons to be left on the site vacated by the removed oxygen. The present first-principles calculations will give an answer to this question, and will also allow us to investigate the states occupied by these electrons.

There have been many spectroscopic measurements of the surface electronic structure of $SnO_2(110)$. The experimental evidence shows that on the stoichiometric surface there are no states in the gap [9]. However, removal of surface oxygen by heating in high vacuum leads to a broad distribution of gap states [9]. The surprising feature is that these gap states appear to extend up in energy from the valence band maximum (VBM). At moderate temperatures of ~ 600 K, there is a weak distribution of states extending to ~ 1.6 eV above the VBM. As the temperature is raised to ~ 1075 K, and more oxygen is lost, a continuous distribution of states spreads up to the Fermi level, which lies just below the conduction band minimum (CBM). This implies that gap states extend almost across the entire gap. This behaviour is surprising because in most materials it is appropriate to consider the F-center states as pulled

down from the CBM by the Coulomb attraction of conduction electrons to the anion vacancy. Indeed, the electron states associated with F-centers in *bulk* SnO_2 are known to lie only ~ 0.15 eV below the CBM [18,19]. An instructive comparison here is with the electronic structure of the (110) surface of TiO_2, which has the same crystal structure as SnO_2. When TiO_2(110) loses oxygen, gap states appear below the CBM, as expected from the simple arguments, the depth of these states below the CBM being ~ 0.8 eV [37–39]. An important purpose of the present work is to shed light on the seemingly anomalous behaviour of SnO_2. As we shall see, our calculations do show a broad distribution of states in the gap for the reduced surface of SnO_2, and we shall be able to identify these surface states as the states occupied by electrons left by removed oxygen. We shall also be able to confirm a conjecture by Cox et al. [5] that the energy of the surface states is strongly influenced by the high polarizability of the Sn^{2+} ion, and we shall suggest a connection with the unusual structure of the SnO crystal, which is also stabilized by this polarizability, as pointed out in our recent paper [32]. So far as we are aware, no previous first-principles work on SnO_2 surfaces has been reported, although there have been two recent papers on the TiO_2 surface [29,40], and we shall discuss the relation between that work and the work reported here. There have been previous attempts to treat the surface properties of SnO_2(110) using non-self-consistent tight-binding methods [15,16], which will also be discussed later.

The rest of the present paper is organized as follows. The following section gives a brief summary of the techniques used in the work. Section 3 then presents our results for the equilibrium structure, energy, valence charge distribution and density of states of the stoichiometric (110) surface. Results for the reduced (110) surface are described in Section 4. Finally, the significance of our results and some pointers to future work are discussed in Section 5.

2. Techniques

The calculations are based on density functional theory and the pseudopotential approximation, with electron correlation described by the local density approximation (LDA). These well established and commonly used techniques have been extensively reviewed in the literature (see e.g. Refs. [20–22]). In the pseudopotential approach, it is assumed that the core orbitals have exactly the same form as in free atoms, and only valence electrons are represented explicitly in the calculations. The valence–core interactions are described by non-local pseudopotentials, which are generated by ab initio calculations on isolated atoms. The solid-state calculations are performed on periodically repeating cells, with occupied valence orbitals represented by a plane-wave expansion. This expansion includes all plane waves whose kinetic energy $E_k = \hbar^2 k^2 / 2m$ (k the wavevector, m the electron mass) satisfies $E_k < E_{cut}$, where E_{cut} is a chosen plane-wave cut-off energy. Convergence of the calculations with respect to the size of basis set is achieved by systematic increase of the plane-wave cut-off E_{cut}.

The present calculations were performed partly using the sequential code CASTEP (Cambridge sequential total energy package) [22] running on the Cray Y-MP at the Rutherford–Appleton Laboratory, and partly with its parallel version CETEP (Cambridge–Edinburgh total energy package) [41] on the 64-node Intel iPSC/860 machine at the Daresbury Laboratory.

The pseudopotentials we use are exactly the same as those used in our earlier work on the SnO_2 and SnO perfect crystals [32]. Briefly, the Sn pseudopotential was generated using the standard Kerker scheme [42], treating the 5s and 5p levels as valence states and the 4d levels and all lower levels as core states. For oxygen, we use a pseudopotential that was carefully optimized using the technique of Lin et al. [43] in order to reduce the plane-wave cut-off as much as possible. Both pseudopotentials are treated in the Kleinman–Bylander (KB) representation [44], with the p-wave treated as local for both elements. The LDA exchange–correlation energy is represented by the Ceperley–Alder formula [45,46], and Brillouin zone sampling is performed using the Monkhorst–Pack scheme [47].

The pseudopotentials, and other aspects of the current techniques, have been thoroughly tested in our earlier work on the SnO_2 and SnO perfect crystals [32], where we made detailed comparisons

with experiment for the equilibrium crystal structures, the zone-center phonon frequencies and the electronic densities of states. We showed there that with the pseudopotentials we are using a plane-wave cut-off of 1000 eV is needed to achieve good convergence, and this is the cut-off used throughout the present work.

3. The stoichiometric (110) surface

A general view of the stoichiometric (110) surface of SnO_2 is shown in Fig. 1. The structure we are assuming here is the one deduced from a wide range of measurements (see e.g. Refs. [9,12,14]). The terminology we shall use when discussing the surface structure is as follows. The outermost ions, which are oxygen ions forming ridges parallel to the c-axis, will be referred to as bridging oxygens. Below these is a plane containing both tin and oxygen ions; the oxygens in this plane will be called in-plane oxygens. The tin ions in this plane occupy two kinds of site, one of which lies below the ridge of bridging oxygens and will be called the bridging tin site. The second kind of tin site is five-fold coordinated on the stoichiometric surface, and we call it the five-fold tin site. Finally, we shall need to refer to the oxygens below this plane, lying vertically beneath bridging oxygens; we call these sub-bridging oxygens.

3.1. Tests of vacuum width

As in our previous work on oxide surfaces [26,27,31], the calculations are done in slab geometry. The use of this geometry is an artifact which we are obliged to use because our electronic structure techniques are based on periodic boundary conditions. Our calculations are performed on a collection of ions in a box having the shape of a parallelepiped, which is periodically repeated in all three directions. The repeating box contains a single unit cell of a slab of ions, and repetition in the plane of the slab has the effect of creating an infinite slab. Repetition in the third direction creates an infinite stack of slabs, each slab being separated from its neighbours by a vacuum layer.

Our real interest is, of course, in the properties of a single surface of a semi-infinite crystal. In order to

be sure that these properties can be obtained by studying repeated slabs, one has to choose the width of the vacuum between slabs, and the thickness of the slabs themselves large enough so that the surfaces have only a negligible effect on each other. Slabs of stoichiometric SnO_2 having (110) surfaces consist of layers containing Sn and O ions (referred to as Sn–O layers), and layers containing only O ions. It is convenient to specify the thickness of such a slab by giving the number of Sn–O layers. The thinnest slab for which we can expect meaningful results consists of two Sn–O layers. We report results both for this system, whose slab unit cell contains 12 ions, and the four-layer system having a unit cell of 24 ions.

We have investigated the effect of vacuum width by performing a series of calculations on the two-layer system. For the purpose of these tests, the ions in each slab are at their unrelaxed perfect-crystal positions. Brillouin zone sampling is performed using the lowest-order Monkhorst–Pack scheme [47], so that the sampling wavevectors are $(\pm \frac{1}{4}, \pm \frac{1}{4}, \pm \frac{1}{4})$ in units of the primitive reciprocal lattice vectors of the repeating cell. We specify the vacuum width L' by the distance between neighbouring slabs measured along the surface normal, defined so that for zero width the stack of slabs becomes identical to the infinite perfect crystal.

For these tests, we wish to know how large the vacuum width has to be for the surface energy σ to be independent of this width. Table 1 shows our calculated values of the unrelaxed surface energy of the two-layer system as a function of L'. The surface energy σ is obtained by subtracting the energy per cell for the case $L' = 0$ from the energy per cell for the L' of interest and dividing by the total surface area per cell. Judging by the dependence of σ on L', one sees that slab interactions across the vacuum width are completely negligible for $L' \geqslant 3.28$ Å, and

Table 1
Calculated energy per unit area of the unrelaxed (110) stoichiometric surface of SnO_2 for different vacuum widths

Vacuum width (Å)	Surface energy (J m^{-2})
1.64	1.68
3.28	1.96
4.92	2.00
6.56	2.00

this is the value of L' we have adopted for all subsequent calculations. The effects of slab *thickness* will become clear as we proceed.

It is useful to note that for thick vacuum layers the energy dispersion of electron states propagating normal to the surface must vanish. This means that there is nothing to be gained from k-point sampling normal to the surface. The Monkhorst–Pack sampling set $(\pm \frac{1}{4}, \pm \frac{1}{4}, \pm \frac{1}{4})$ can therefore be replaced by the set $(0, \pm \frac{1}{4}, \pm \frac{1}{4})$ without making any difference. We have checked that this is indeed the case for the vacuum width of 3.28 Å.

3.2. The relaxed structure and the valence charge density

We have performed calculations of the equilibrium relaxed structure for both the two-layer and four-layer systems. Relaxation has been performed using the steepest descents method, the criterion for equilibrium being that the forces on all atoms should be less than 0.4 eV Å^{-1}. This criterion is enough to ensure that further reduction would change the surface energy by less than 0.01 J m^{-2} and the ionic positions by less than 0.01 Å; these changes are negligible for practical purposes.

Relaxation of the two-layer system causes the surface energy to decrease from 1.96 to 1.35 J m^{-2}. For the four-layer system, the relaxed surface energy is 1.50 J m^{-2}. The difference between these two values is not entirely negligible, and it is clear that interactions between the surfaces are significant for
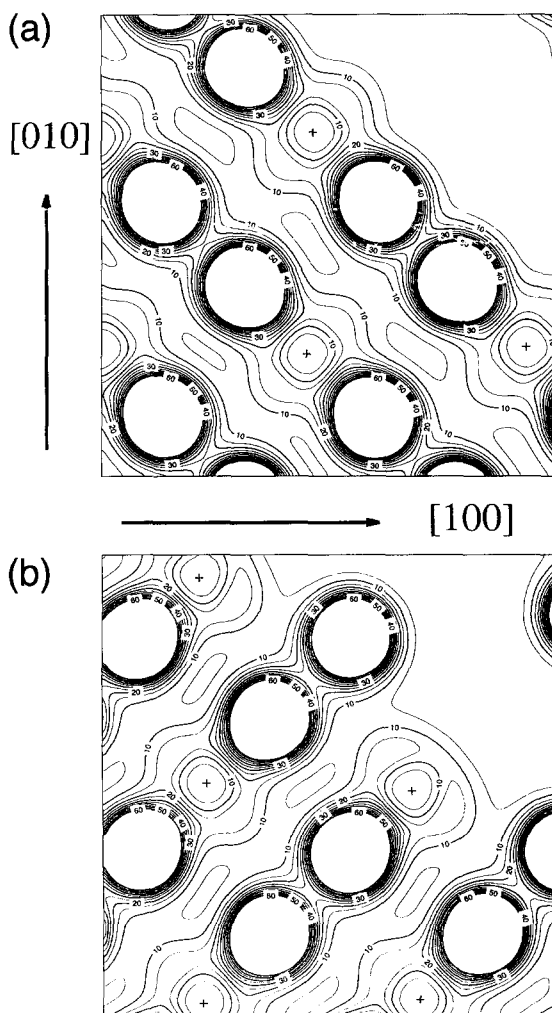
Table 2
Relaxed positions of ions at the stoichiometric surface

Atoms	No. of layers	Δx (Å)	Δy (Å)
Bridging tins	2	+0.26	–
Bridging tins	4	+0.15	–
5-fold tins	2	−0.21	–
5-fold tins	4	−0.15	–
Bridging oxygens	2	+0.11	–
Bridging oxygens	4	+0.02	–
In-plane oxygens	2	+0.11	+0.05
In-plane oxygens	4	+0.07	+0.05

Calculated values are given for the displacements of the ions from their perfect-lattice positions for the two-layer and four-layer slabs. Cartesian components of the displacements are given along the surface normal (110) direction (Δx) and along the (1$\bar{1}$1) direction (Δy). Dashes indicate values that are zero by symmetry. The nomenclature for surface ions is explained in the text.

Fig. 2. Contour plots of valence electron density (units: 10^{-2} electron/Å^3) on (001) planes passing through the slabs used for studying the stoichiometric (panels (a) and (b)), fully reduced ((c) and (d)) and half-reduced ((e) and (f)) (110) surfaces. For each surface, two planes are shown, passing through the in-plane oxygen and bridging tin sites ((a), (c), (e)) and the bridging oxygen and fivefold tin sites ((b), (d), (f)). Regular Sn sites are marked by the symbol ×.

the two-layer slab. So far as we are aware, there are no experimental values for the surface energy of SnO_2. However, it is interesting to note that the calculations of Mulheran and Harding [17] based on an empirical interaction model for SnO_2 gave the value of 1.38 J m^{-2} for the (110) surface.

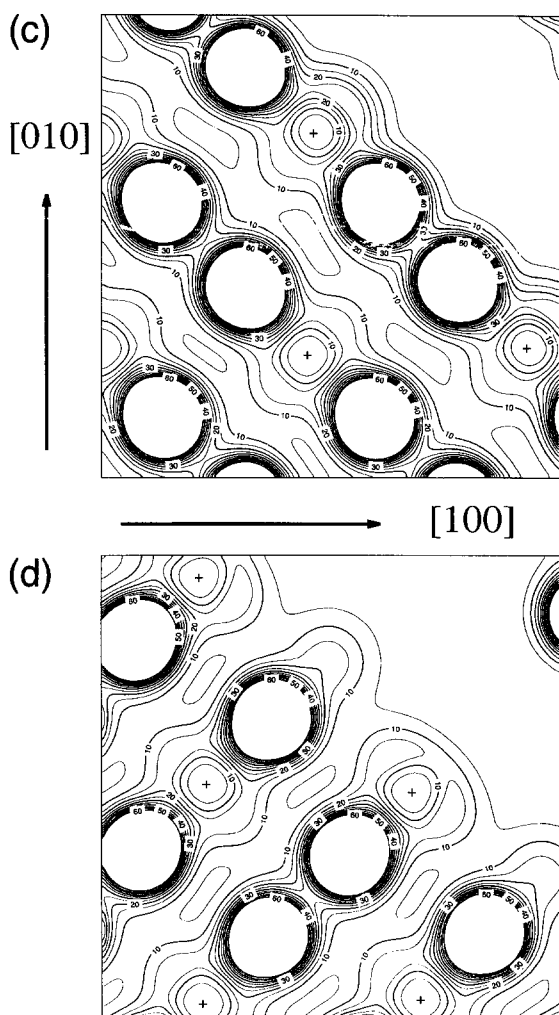Table 2 shows the displacements of the surface Sn and O ions away from their perfect-crystal positions

(c)

[010]

[100]

(d)

Fig. 2 (continued).

MgO(001). Secondly, there are significant differences between the results for the two slabs. In all cases, the displacements are smaller for the thicker slab, and this explains why the relaxed surface energy is slightly higher for the 4-layer slab. The indication is that relaxations at the two surfaces are interacting significantly with each other in the 2-layer slab, and that this slab is not fully adequate for quantitative calculations. However, the sign and general magnitude of the displacements are the same for both slabs. More discussion of the displacements will be given in Section 5.
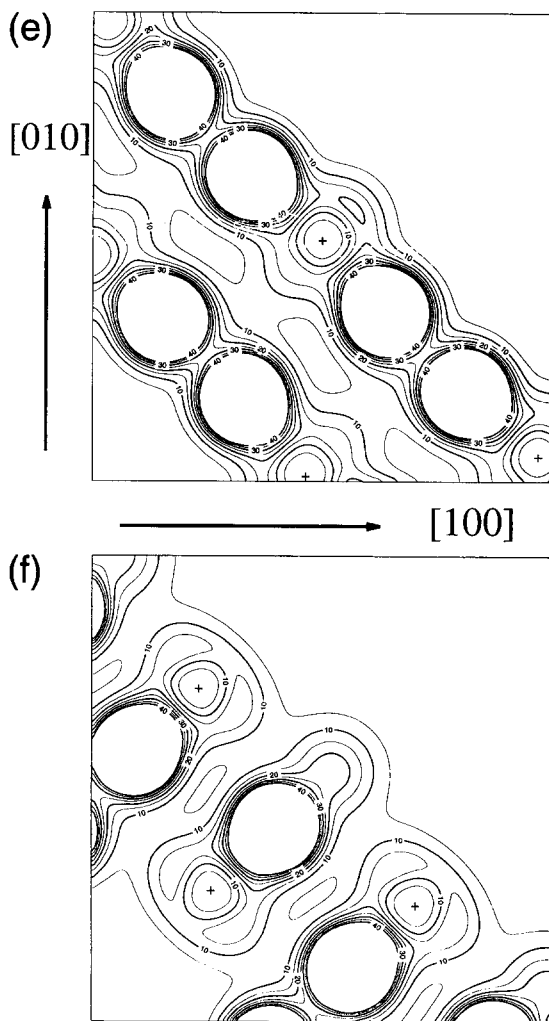
We show in Fig. 2 the valence electron density on

(e)

[010]

[100]

(f)

Fig. 2 (continued).

for both the two-layer and four-layer slabs. For both the five-fold and bridging Sn ions and for the bridging O ion, the relaxations are along the surface normal, i.e. the (110) direction, by symmetry. For the in-plane O ion, relaxations along both the (110) and ($1\bar{1}0$) directions are possible. Relaxations are counted positive if they are along the outward normal, and for in-plane O, displacements along ($1\bar{1}0$) are positive if the ion moves away from the neighbouring bridging Sn.

Two conclusions emerge from this table. Firstly, the displacements of surface ions are substantial, compared with the relaxations at inert surfaces like

two (001) planes which both pass through Sn and O sites. The remarkable feature of these plots is the almost total absence of disturbance of the density in
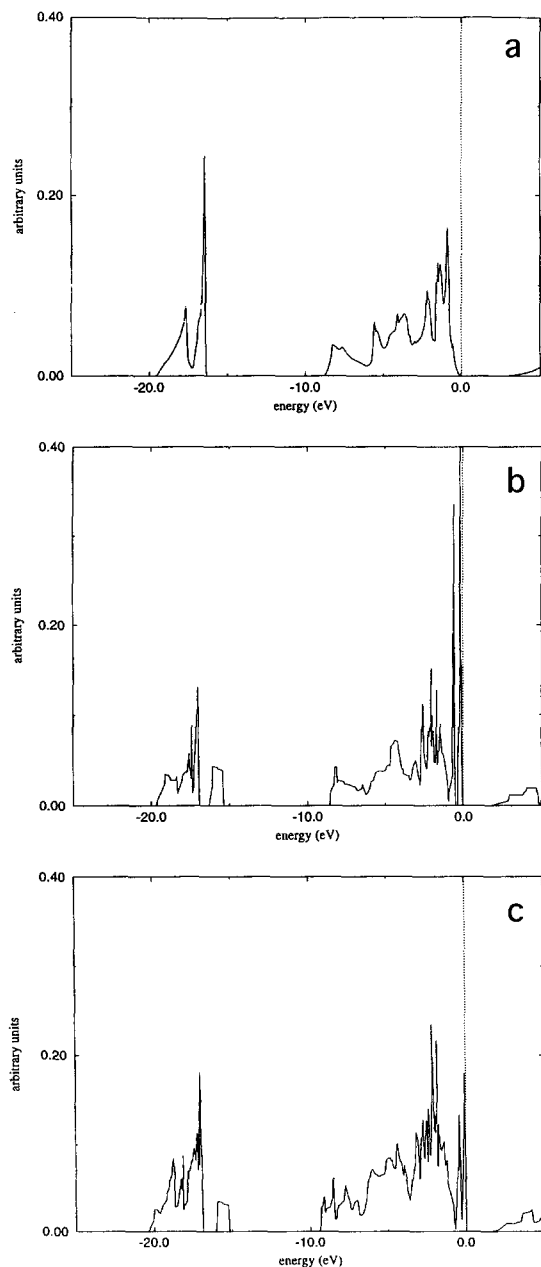

Fig. 3. Electronic DOS for the perfect crystal (a), the two-layer stoichiometric (b) and four-layer stoichiometric (c) slabs, the two-layer fully reduced (d) and four-layer fully reduced (e) slabs, and the two-layer half-reduced slab (f). In all cases, the dashed line marks the energy of the highest occupied state.
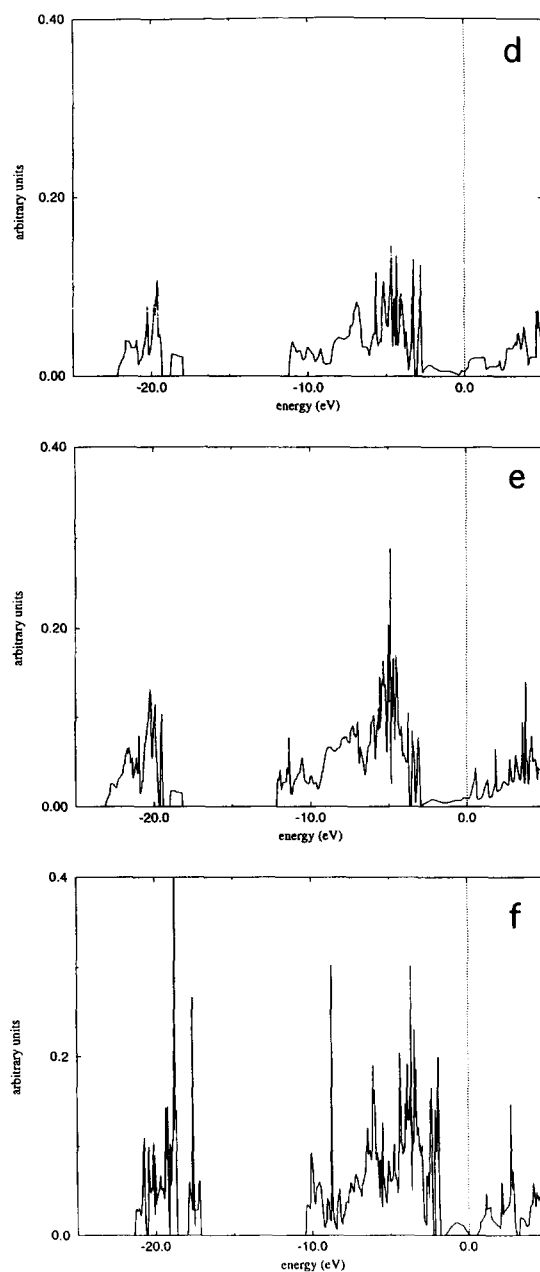

Fig. 3 (continued).

the region away from the surface. We shall refer to these plots again when we discuss the non-stoichiometric surface.

3.3. Electronic structure

We have calculated the electronic density of states (DOS) of the relaxed two-layer and four-layer systems. As with our calculations on the DOS of the perfect crystal [32], we have used the tetrahedron method to perform the integration over the Brillouin zone. (In fact, since k-point sampling is unnecessary along the surface normal, we sample only over the *surface* Brillouin zone, so that the tetrahedron method reduces to the triangle method.) It should be stressed that for systems of the size treated here the calculations are very demanding, and the Brillouin zone sampling we have been able to achieve is rather restricted. We have needed to limit the sampling to only nine points in the irreducible wedge of the surface Brillouin zone, and the energy resolution that this gives is limited.

The calculated DOS for the two sizes of slab are compared with the bulk DOS obtained in our earlier work in Fig. 3. As expected, there is a close similarity between the bulk and slab DOS. However, there are three important differences. Firstly, the slabs exhibit new structure at the top of the valence band, in the form of a pair of sharp peaks. Secondly, there is a slight reduction in the width of the gap. The calculated gap for the bulk is 2.2 eV (experimental value is 3.6 eV [1]), while for the thin and thick slab systems we find gaps of 1.6 and 1.5 eV respectively. The new peaks at the VBM appear to be mainly responsible for the narrowing of the gap. The third difference is that in the slab system states split off from the top of the O(2s) band.

We have studied the states at the top of the valence band in some detail. Examination of the eigenvalues shows that there are two states per repeating cell associated with each of the sharp peaks at the VBM. To analyze the nature of these states, we have calculated the electronic density $\rho_i(r)$ of each of these states separately. This density is defined as

$$\rho_i(r) = \sum_k w_k \mid \psi_{ik}(r) \mid^2, \tag{1}$$

where the sum goes over sampling vectors in the irreducible wedge, w_k is a sampling weight, and $\psi_{ik}(r)$ is the normalized wave function of state i at sampling vector k.
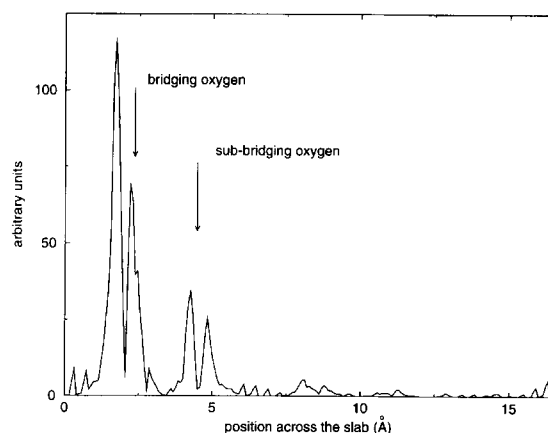

Fig. 4. Plot of electronic density associated with the two states in the first peak at the top of the valence band in the four-layer stoichiometric slab. The line on which the density is plotted passes through the bridging and sub-bridging oxygen sites, which are marked by arrows.

We find that all four states are quite strongly localized on bridging oxygens, with some weight also on sub-bridging oxygens; the weight on in-plane atoms and elsewhere in the slab is small. One of the states associated with each DOS peak can be regarded as being localized at one of the surfaces of the slab. To illustrate the localization of the states, we show in Fig. 4 a plot of the sum of the densities $\rho_i(r)$ associated with the two states responsible for the first peak at the VBM. This shows the rather rapid decrease of density as one passes into the slab along the surface normal through the bridging oxygen. Detailed examination of density contour plots (not shown here) indicates that the states associated with the two peaks have different symmetries. The states of lower energy have mainly p-like character, with the axis along the surface normal. The higher states are also p-like, but with the axis along the $(1\bar{1}0)$ direction, in other words perpendicular to the rows of bridging oxygens.

Although most of the reduction of the band gap is due to the localized states at the VBM, there is some indication of a small contribution to the reduction from states at the CBM. This indication comes from examination of $\rho_i(r)$ for the two lowest states of the conduction band, which show some localization in the surface region.

The peak in the DOS split off from the O(2s) band contains two states per cell. Plots of $\rho_i(r)$

show that these states are strongly localized on the bridging oxygens, with some weight on the sub-bridging oxygens. The form of $\rho_i(r)$ confirms the expected s-like character of these states.

4. The reduced (110) surface

4.1. The relaxed structure and valence charge density

All the experiments indicate that reduction of the (110) surface occurs by removal of bridging oxygens. However, it is also clear that the fraction of bridging oxygens removed depends on the conditions. We have investigated two cases: first, the case where all bridging oxygens are removed (referred to as fully reduced), and second, the case where only half of them are removed (half reduced). We have studied the fully reduced surface using both the two-layer and four-layer slabs. To study the half-reduced case, we have treated the situation where every other bridging oxygen is removed, so that we have an ordered array of surface vacancies. For this case, the surface unit cell has to be doubled along the c-axis, and at present we can only handle this with the two-layer slab. Views of the two reduced surfaces are shown in Fig. 1. It is important to stress that we create the reduced surface by removing oxygen from one surface of the slab only; the other surface remains stoichiometric.

The ionic relaxations for the fully relaxed surface are reported in Table 3. It is extremely remarkable that the displacements of the ions near the surface are almost identical to those we have found at the

Table 3
Relaxed positions of ions at the fully reduced surface

Atoms	No. of layers	Δx (Å)	Δy (Å)
Bridging tins	2	+0.24	–
Bridging tins	4	+0.23	–
5-fold tins	2	−0.17	–
5-fold tins	4	−0.18	–
In-plane oxygens	2	+0.09	+0.07
In-plane oxygens	4	+0.08	+0.07

Cartesian components of displacements away from perfect-lattice positions are given, following the notation and nomenclature of Table 2.

Table 4
Relaxed positions of ions at the half-reduced surface

Atoms	Δx (Å)	Δy (Å)	Δz (Å)
Bridging tins	+0.27	–	+0.03
5-fold tins (1)	−0.23	–	–
5-fold tins (2)	−0.24	–	–
Bridging oxygens	+0.13	–	–
In-plane oxygens	+0.11	+0.04	0.00

Cartesian components of displacements away from perfect-lattice positions are given, following the notation and nomenclature of Table 2. The displacement component denoted by Δz is along the (001) direction.

stoichiometric surface (see Table 2). This strongly suggests that the electrons left at the surface by the removal of oxygen are exerting roughly the same forces as the original bridging oxygens. In Table 4, we show the ionic relaxations for the half-reduced surface. In this case, because of the lower symmetry, the ionic displacements can have components in directions for which they were zero by symmetry at the fully reduced surface. Comparison of these results with those for the 2-layer stoichiometric slab (Table 2) shows that the displacements are almost identical in the two cases. This indicates once again that removal of bridging oxygen leads to surprisingly small adjustments of the ionic positions.

The valence charge density of the relaxed fully reduced four-layer slab is shown in Fig. 2 on the same two (001) planes for which we showed the charge density of the stoichiometric surface. Comparing the two pairs of plots, we see a very large change of density distribution in the immediate neighborhood of the removed bridging oxygen and the bridging tin directly below it. The extreme localization of this disturbance is very striking. Not only is the density completely unaltered on atomic layers immediately below the surface, but even around the in-plane oxygen and five-fold tin sites there is no visible change. It appears that the two electrons per bridging oxygen left on the surface are localized in channels running along the (001) direction just above the bridging tin sites and passing through the bridging oxygen positions. This will be confirmed in greater detail when we discuss the electronic structure below.

The valence distribution at the half-reduced surface is also shown in Fig. 2. The main differences

with the plots for the fully reduced surface are that the electron density is now lower near the bridging Sn site and greater near the empty bridging oxygen

Fig. 5. Contour plots of electron density (units: electrons/Å³) associated with the single state (per removed oxygen) spanning the band-gap for the four-layer fully reduced slab. Plots are on (001) planes passing through the bridging tin and in-plane oxygen sites (panel (a)) and bridging and sub-bridging oxygen sites (b). Intersections of the guide lines mark the significant sites: in panel (a) the intersection below the centre is the bridging tin, and the intersections on either side are in-plane oxygens; in panel (b), the intersection at the centre is the bridging oxygen site and the lower intersection is sub-bridging oxygen. Distances are in Å.

site. This is what we should expect, since the surface electrons are now more strongly confined between the remaining bridging oxygens.

4.2. Electronic structure

The calculated densities of states for the two-layer and four-layer fully reduced systems and for the two-layer half-reduced system are shown in Fig. 3. The major change from the stoichiometric system is the appearance of broad distributions of states in the band gap. For the fully reduced case, the states span the whole gap, but for the half-reduced system there is a band of gap states roughly in the middle of the gap. We also note the two sharp peaks at the VBM and the peak split off from the O(2s) band that we found for the stoichiometric surface. Since bridging oxygens have been removed only from one side of the slab, we clearly expect these states to remain unchanged on the other surface. This implies that there should be one state in each of these peaks, and we have verified that this is the case.

We find that there is a single state responsible for the part of the DOS spanning the gap. The variation of the energy of this state with k-vector is responsible for the spread in energy. Density plots of $\rho_i(r)$ for this state show that it is strongly localized in the surface region near the bridging tin and oxygen sites. Contour plots of $\rho_i(r)$ on (001) planes passing through this site and through the bridging tin site are shown in Fig. 5. The plots show that there are substantial concentrations of density in the region vertically above the bridging tin site, on in-plane oxygens and on the sub-bridging oxygens. Integration of the density in these features shows that roughly 30% is in the region above the tin site, 10% on each of the in-plane oxygens, 10% on sub-bridging oxygen, and the remainder in small features elsewhere.
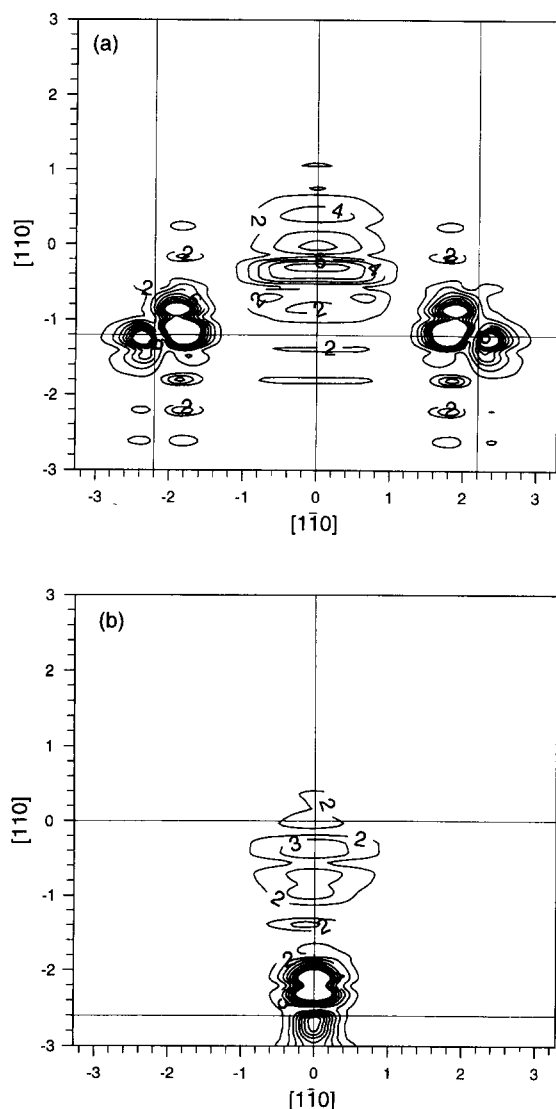
5. Discussion

In assessing our results, it is important to bear in mind the strengths and weaknesses of density functional theory, which forms the basis of all our calculations. DFT is a theory of the ground state, and we expect it to give an accurate description of the

energetics of the system in the ground state, which in the present case includes surface energies and the equilibrium positions of the atoms in the relaxed surface. The theory is also designed to give accurate results for the valence electron distribution, and for related quantities such as the distribution of electrostatic potential. On the other hand, the principles of DFT give us no right to expect accurate results for excited-state properties. It is well known, for example, that DFT generally underestimates band gaps. As we reported in our previous paper [32], our calculated band gap for bulk SnO_2 is 2.2 eV, which is ~ 40% smaller than the experimental value of 3.6 eV. One therefore needs to be more cautious about the interpretation of excited-state results. Nevertheless, it has been found that DFT does usually give a reliable semiquantitative guide to electronic densities of states, and we shall certainly draw important conclusions from our results for such quantities.

We have shown that atomic relaxations at both the stoichiometric and reduced (110) surfaces are rather moderate, being on the order of 0.1–0.3 Å. This is large compared with the very tiny displacements on the MgO(001) surface [31,33–36], but small compared with the giant displacements at the α-Al_2O_3 basal-plane surface [26,27]. We find that five-fold coordinated Sn moves into the surface, while bridging Sn and in-plane O move out. The separation between bridging O and bridging Sn decreases markedly. These qualitative features are the same as found by Ramamoorthy et al. [29] in their DFT–pseudopotential calculations on the TiO_2(110) surface, and the magnitudes of their displacements are also very similar to ours. The only significant difference is that the absolute displacement of bridging O in TiO_2 is inwards, whereas we find it be outwards for SnO_2. Independent DFT calculations on TiO_2(110) have also been performed by Vogtenhuber et al. [40] using the FLAPW technique. These authors find qualitatively similar results.

Relaxation has a significant effect on the surface energy, reducing it from 1.96 to 1.50 J m^{-2} for the stoichiometric surface. This relaxed surface energy is quite close to the value of 1.38 J m^{-2} calculated by Mulheran and Harding [17] using an empirical interaction model. This provides support for the realism of the ionic model they use [49]. Unfortunately, Mulheran and Harding do not report results for the

surface relaxations they obtain with the model. It is also worth noting that our calculated surface energy is rather similar to the value of 0.9 J m^{-2} found by Ramamoorthy et al. for the relaxed TiO_2(110) surface.

On both the stoichiometric and reduced surfaces, we find marked changes of electronic structure compared with the bulk. The rather well localized surface states on bridging oxygen that we have found on the stoichiometric surface are not unexpected. These states, both above the O(2s) band and at the VBM are localized largely on bridging oxygen, which is in an exposed position where one would expect a reduced Madelung potential and hence a reduction in the binding of states. So far as we are aware, there is at present no experimental evidence for the existence of surface O(2s) states. Detailed UPS measurement have been performed on the stoichiometric SnO_2(110) surface, and no evidence has been found for surface states at the VBM. Because of this rather surprising disagreement, we have tested the robustness of this aspect of our calculations by repeating them with an independently generated pseudopotential, but this makes no difference. It is conceivable that the problem might arise from our treatment of the Sn(4d) states as core states, or even from deficiencies of the LDA, but it would require a substantial effort to test either of these possibilities.

At the reduced surface, we have shown that the two electrons left by the removal of neutral oxygen occupy surface states localized in the region of the empty bridging oxygen sites and the adjacent bridging tin sites. More accurately, their density is concentrated immediately above the bridging tin atoms, with some weight on in-plane oxygens and elsewhere. This finding provides direct support for the common assumption that oxygen loss leads to reduction of tin from Sn^{4+} to Sn^{2+}. However, our results make it clear that if one does wish to use the Sn^{2+} description, then it is crucial to recognize the extreme distortion of this ion. The change of electron density caused by reduction occurs entirely on the vacuum side of the bridging Sn ions, which, if considered as Sn^{2+} ions, must be regarded as maximally polarized. A high degree of polarization of these ions is expected, because they are very polarizable, and oxygen removal makes their invironment very unsymmetrical. Their high polarizability arises

from the rather small energy difference between 5s and 5p states and the large spatial overlap of these states. As emphasized in our earlier paper [32], the Sn^{2+} ion in the SnO perfect crystal is also in a very unsymmetrical environment, and we showed that there also the Sn ion exhibits maximal polarization. It would be interesting to know the valence charge distribution at the reduced TiO_2 surface, but this appears not to have been examined in the first-principles calculations of Ramamoorthy et al. [29,30]. The lowest-lying conduction-band states in that case have Ti(3d) character, and the weak spatial overlap between 3d and 4p states will make the reduced Ti ion much less polarizable. The surface charge distribution of TiO_2 should therefore be rather different from that of reduced SnO_2.

On the fully reduced surface, we find a broad band of surface states spanning the entire gap, and we have demonstrated that occupation of these states is responsible for the surface electron density above bridging Sn sites. On the half-reduced surface, the band of gap states contracts to have a width of ~ 1.5 eV, and lies ~ 1.1 eV above the VBM. In comparing with experiment, it must be remembered that the real surface is likely to be significantly disordered. Experimentally [9], a weak distribution of states near the bottom of the gap is observed for small degrees of reduction. As further oxygen is removed, the distribution spreads upwards to the Fermi level, which is just below the top of the gap. It seems clear that these must be essentially the same as the gap states we find.

The large width of the band of gap states is not surprising, since the electrons in these states are able to propagate almost freely along the c-axis. The width of ~ 1.5 eV we find for the half-reduced surface is also reasonable. It is interesting to note that recent calculations on periodic arrays of F-centers in bulk MgO [50] find a band width of gap states of 1.6 eV when the spacing between F-centers is 5.9 Å, and the F-center states have been found to have a substantial amplitude on neighboring oxygens. The energy of the gap state is also understandable, following an argument originally due to Cox et al. [5]. We have seen that the Sn^{2+} ions are highly polarized. This must arise from a strong mixing of the 5s and 5p states caused by surface fields, and this mixing will displace one of the hybrid states down-

wards in energy. Alternatively, we can adopt the F-center viewpoint and note that F-center levels are commonly found rather deep in the gap. For example, in bulk MgO the F-center levels are roughly 5 eV below the CBM. In very recent DFT calculations, we have found that surface F-centers in MgO have their levels at almost the same energy as as those in the bulk [51]. This still leaves an unresolved question, however, concerning the relation between bulk and surface F-centers in SnO_2. It is rather well established that the donor states involved in n-type SnO_2 are oxygen vacancies, and that the binding energy of electrons to these vacancies is no more than ~ 0.15 eV [18,19]. This implies that bulk and surface F-centers in SnO_2 must have very different properties, and the reasons for this need to be explored. We hope to return to this question in the future.

The insights we have gained allow us to comment on the predictions of tight-binding calculations. The recent tight-binding work of Godin and LaFemina [16] made a thorough investigation of the stoichiometric and fully reduced $SnO_2(110)$ surfaces. No states were found in the gap for either surface. This was consistent with previous tight-binding work of Munnix and Schmeits [15], who studied oxygen vacancies on the $SnO_2(110)$ surface and found no gap states. These results are in conflict with what we have found. It is also noteworthy that tight-binding calculations on the $TiO_2(110)$ surface [52] failed to find any gap states associated with oxygen vacancies, even though the existence of such states has been well established for many years [37–39]. In our view, the tight-binding models used in the above work lack an essential piece of physics. We have argued from our results that if one adopts an LCAO viewpoint then Sn^{2+} states are crucially influenced by cation s–p mixing caused by surface fields. But such a mechanism is completely lacking from the tight-binding models used in the above work. There is no term in the Hamiltonian which accounts for this mechanism of s–p mixing, and no inclusion of any kind of effect arising from surface fields. Very recently, self-consistent tight-binding calculations on $TiO_2(110)$ and other oxide surfaces have been reported, in which Coulombic effects are approximately included [53,54]. Although only the stoichiometric surface has been studied so far by these

methods, it is already clear from these papers that self-consistency has a major effect on the surface electronic states.

Finally, we note that much of the practical interest in SnO_2 surfaces centers on the adsorption and reactions of molecules. We are currently using the results of the present work as a basis for investigating the dissociation of H_2O at the $SnO_2(110)$ surface [55], and we hope to report on this soon.

Acknowledgements

References

[1] V.T. Agekyan, Phys. Status Solidi (a)43 (1975) 11.
[2] J.F. McAleer, P.T. Moseley, J.O.W. Norris and D.E. Williams, J. Chem. Soc. Faraday Trans. I 83 (1987) 1323; 84 (1988) 441.
[3] I. Brown and W.R. Patterson, J. Chem. Soc. Faraday Trans. I 79 (1983) 1431.
[4] E. de Frésart, J. Darville and J.M. Gilles, Solid State Commun. 37 (1980) 13.
[5] P.A. Cox, R.G. Egdell, C. Harding, W.R. Patterson and P.J. Tavener, Surf. Sci. 123 (1982) 179.
[6] R.G. Egdell, S. Eriksen and W.R. Flavell, Solid State Commun. 60 (1986) 835.
[7] R.G. Egdell, S. Eriksen and W.R. Flavell, Surf. Sci. 192 (1987) 265.
[8] J.W. Erickson and S. Semancik, Surf. Sci. 187 (1987) L658.
[9] D.F. Cox, T.B. Fryberger and S. Semancik, Phys. Rev. B 38 (1988) 2072.
[10] D.F. Cox, T.B. Fryberger and S. Semancik, Surf. Sci. 224 (1989) 121.
[11] D.F. Cox and T.B. Fryberger, Surf. Sci. 227 (1990) L105.
[12] J.M. Themlin, R. Sporken, J. Darville, R. Caudano, J.M. Gilles and R.L. Johnson, Phys. Rev. B 42 (1990) 11914.
[13] G.L. Shen, R. Casanova, G. Thornton and I. Colera, J. Phys. Condens. Matter 3 (1991) S291.
[14] R.G. Egdell, in: The Science of Ceramic Interfaces II, Ed. J. Nowotny (Elsevier, New York, 1994) p. 527.
[15] S. Munnix and M. Schmeits, Phys. Rev. B 27 (1983) 7624; 33 (1986) 4136.
[16] T.J. Godin and J.P. LaFemina, Phys. Rev. B 47 (1993) 6518.
[17] P.A. Mulheran and J.H. Harding, Mod. Sim. Mater. Sci. Eng. 1 (1992) 39.
[18] J.A. Marley and R.C. Dockerty, Phys. Rev. 140 (1965) A304.
[19] S. Samson and C.G. Fonstad, J. Appl. Phys. 44 (1973) 4618.
[20] G.P. Srivastava and D. Weaire, Adv. Phys. 36 (1987) 463.
[21] M.J. Gillan, in: Proc. NATO ASI on Computer Simulation in Materials Science, Aussois, March 1991, Eds. M. Meyer and V. Pontikis (Dordrecht, Kluwer, 1991) p. 257.
[22] M.C. Payne, M.P. Teter, D.C. Allan, T.A. Arias and J.D. Joannopoulos, Rev. Mod. Phys. 64 (1992) 1045.
[23] A. De Vita, M.J. Gillan, J.-S. Lin, M.C. Payne, I. Štich and L.J. Clarke, Phys. Rev. Lett. 68 (1992) 3319.
[24] A. De Vita, M.J. Gillan, J.-S. Lin, M.C. Payne, I. Štich and L.J. Clarke, Phys. Rev. B 46 (1992) 12964.
[25] I. Manassidis, A. De Vita, J.-S. Lin and M.J. Gillan, Europhys. Lett. 19 (1992) 605.
[26] I. Manassidis, A. De Vita and M.J. Gillan, Surf. Sci. 285 (1993) L517.
[27] I. Manassidis and M.J. Gillan, J. Am. Ceram. Soc. 77 (1994) 335.
[28] N. Binggeli, J.R. Chelikowsky and R.M. Wentzcovitch, Phys. Rev. B 49 (1994) 9336.
[29] M. Ramamoorthy, R.D. King-Smith and D. Vanderbilt, Phys. Rev. B 49 (1994) 7709.
[30] M. Ramamoorthy, D. Vanderbilt and R.D. King-Smith, Phys. Rev. B 49 (1994) 16721.
[31] S. Pugh and M.J. Gillan, Surf. Sci. 320 (1994) 331.
[32] I. Manassidis and M.J. Gillan, Phys. Rev. B, submitted.
[33] M.R. Welton-Cook and W. Berndt, J. Phys. C 15 (1982) 5691.
[34] D.L. Blanchard, D.L. Lessor, J.P. LaFemina, D.R. Baer, W.K. Ford and T. Guo, J. Vac. Sci. Technol. A 9 (1991) 1814.
[35] T. Urano, T. Kanaji and M. Kaboragi, Surf. Sci. 134 (1983) 109.
[36] M. Causà, R. Dovesi, C. Pisani and C. Roetti, Surf. Sci. 175 (1986) 551.
[37] V.E. Henrich, G. Dresselhaus and H.J. Zeiger, Phys. Rev. Lett. 36 (1976) 1335.
[38] K.E. Smith, J.L. Mackay and V.E. Henrich, Phys. Rev. B 35 (1987) 5822.
[39] R.L. Kurtz, R. Stockbauer, T.E. Madey, E. Román and J.L. de Segovia, Surf. Sci. 218 (1989) 178.
[40] D. Vogtenhuber, R. Podloucky, A. Neckel, S.G. Steinmann and A.J. Freeman, Phys. Rev. B 49 (1994) 2099.
[41] L.J. Clarke, I. Štich and M.C. Payne, Comput. Phys. Commun. 72 (1992) 14.

[42] G.P. Kerker, J. Phys. C 13 (1980) L189.

[43] J.-S. Lin, A. Qteish, M.C. Payne and V. Heine, Phys. Rev. B 47 (1993) 4174.

[44] L. Kleinman and D.M. Bylander, Phys. Rev. Lett. 48 (1980) 566.

[45] D.M. Ceperley and B.J. Alder, Phys. Rev. Lett. 45 (1980) 566.

[46] J. Perdew and A. Zunger, Phys. Rev. B 23 (1981) 5048.

[47] H.J. Monkhorst and J.D. Pack, Phys. Rev. B 13 (1976) 5188.

[48] A.M. Rappe, J.D. Joannopoulos and P.A. Bash, J. Am. Chem. Soc. 114 (1992) 6466.

[49] C.M. Freeman and C.R.A. Catlow, J. Solid State Chem. 85 (1990) 65.

[50] Q.S. Wang and N.A.W. Holzwarth, Phys. Rev. B 41 (1990) 3211.

[51] L.N. Kantorovich and M.J. Gillan, Surf. Sci., submitted.

[52] S. Munnix and M. Schmeits, Phys. Rev. B 31 (1985) 3369; J. Vac. Sci. Technol. A 5 (1987) 910.

[53] J. Goniakowski and C. Noguera, Surf. Sci. 323 (1995) 129.

[54] N. Yu and J.W. Halley, University of Minnesota Supercomputer Institute Research Report UMSI 94/129 (1994).

[55] J. Goniakowski and M.J. Gillan, unpublished.